

1 **Assessing the impact of road segment obstruction on accessibility to**  
2 **critical services in case of a hazard**

3 Sophie Mossoux<sup>1,2</sup>, Matthieu Kervyn<sup>1</sup>, Frank Canters<sup>2</sup>

4

5

6 <sup>1</sup>Physical Geography, Department of Geography, Earth System Science, Vrije Universiteit Brussel, Pleinlaan 2,

7 1050 Brussels, Belgium

8 <sup>2</sup>Cartography and GIS Research Group, Department of Geography, Vrije Universiteit Brussel, Pleinlaan 2, 1050 Brussels,

9 Belgium

10

11 *Correspondence to:* Frank Canters (frank.canters@vub.be)

12

13

14

15

16

17

18

19

20

21

22

23

24

25

26

27

28

29

30

31

32

33

34 **Abstract**

35 Development of hazard maps is one of the measures promoted by the international community to reduce risk. Hazard maps  
36 provide information about the probability of given areas to be affected by one or several hazards. As such they are useful tools  
37 to evaluate risk and support the development of safe policies. So far studies combining hazard mapping with accessibility to  
38 services are few. In hazardous environments, accessibility of the population to strategic infrastructure is important because  
39 emergency services and goods will principally be offered at or provided from these locations. If a road segment is blocked by  
40 a hazard, accessibility to services may be affected, or worse, people may be completely disconnected from specific services.  
41 The importance of each road segment in the transport network as a connecting element enabling access to relevant services is  
42 therefore critical information for the authorities. In this study, we propose a new application of hazard mapping which aims to  
43 define the importance of each road segment in the accessibility to services, taking in account the probability of being affected  
44 by a hazard. By iteratively removing one segment after the other from the road network, changes in accessibility to critical  
45 infrastructure are evaluated. Two metrics of road segment importance considering the population affected and the hazard  
46 probability are calculated for each segment: a road accessibility risk metric and a users' path vulnerability metric. Visualization  
47 of these road metrics is a useful way of valuing hazard maps and may help to support discussions about the development of  
48 new infrastructure, road capacity increase and maintenance of existing infrastructures, and evacuation procedures.

49  
50  
51  
52  
53  
54  
55  
56  
57  
58  
59  
60  
61  
62  
63  
64  
65  
66  
67

## 68 1. Introduction

69 A well-developed transport network is essential to the smooth running of a country since it plays an important role in supporting  
70 social and economic activities (Hong et al., 2015; Jenelius et al., 2006; Mattsson and Jenelius, 2015; Nagurney and Qiang,  
71 2012). A reliable road network is even more important in a hazardous environment where the connection of villages to strategic  
72 infrastructures such as hospitals, fire stations, and commercial and employment centres must be guaranteed, particularly when  
73 a hazard occurs. Even if roads are considered as essential infrastructure, the road network is often designed to function close  
74 to maximum capacity to minimize the costs, with small margins of reserve capacity and little redundancy (Mattsson and  
75 Jenelius, 2015; Taylor et al., 2006). It is therefore sensitive to potential disruptions and its interdependencies with other systems  
76 can lead to serious consequences for the functioning of society and economic activities (Hong et al., 2015; Mattsson and  
77 Jenelius, 2015).

78 Given the functional value of the road network, studies have been conducted to assess road network related vulnerability to a  
79 disruption from different points of view. Some metrics have been proposed to characterize vulnerability of the population to  
80 road disruptions at different administrative levels (e.g. municipalities, states) (Jenelius et al., 2006) and accessibility to main  
81 road axes before and after the occurrence of a natural hazard (Sohn, 2006; Taylor and Susilawati, 2012). Other studies assess  
82 the robustness of the road network as a whole, defined as the degree to which the system can function correctly according to  
83 its design specifications in the presence of serious disruptions (Bil et al., 2014; Chang and Nojima, 2001; Immers et al., 2004;  
84 Institute of Electrical and Electronics Engineers, 1990; Nagurney and Qiang, 2012; Sullivan et al., 2010). At a more local  
85 scale, previous research has characterized vulnerability at the level of individual road segments. In these studies potential  
86 degradation of the road transport system caused by interruption of a specific road segment and its impacts on society is analyzed  
87 (Jenelius and Mattsson, 2015). Through several metrics, studies have evaluated the direct physical, economic and functional  
88 impacts of a road segment disruption (Blake et al., 2017; Pregolato et al., 2017; Winter et al., 2016) as well as indirect impacts,  
89 by analyzing how users adapt their way of travelling in case of a disruption (Bil et al., 2014; Jenelius and Mattsson, 2015;  
90 Postance et al., 2017; Taylor et al., 2006).

91 Several types of disruption can lead to a road failure (e.g. accidents, technical failures, hazards or antagonistic actions). Natural  
92 hazards, events such as floods (e.g. Hong et al., 2015; Sohn, 2006), landslides (e.g. Postance et al., 2017), earthquakes (e.g.  
93 Chang and Nojima, 2001; Peeta et al., 2010), ash fall (e.g. Blake et al., 2017) or lava flows, can cause serious perturbation as  
94 roads may be interrupted or road conditions may deteriorate (Mattsson and Jenelius, 2015). Road disruptions are often  
95 integrated in hazard studies through scenarios which focus on specific locations of the network. In such approach, hazards may  
96 be modelled within administrative entities based on the selection of one possible scenario (Hong et al., 2015; Mattsson and  
97 Jenelius, 2015). Other studies define the road segments that are most susceptible to be affected depending on their location  
98 relative to historical hazard zones (Sohn, 2006) or their closeness to areas having a high susceptibility to host a hazard (Postance  
99 et al., 2017). Probabilistic hazard maps provide relevant information about the probability of given areas to be affected by a  
100 hazard and methods to produce such maps have developed significantly over the last years (e.g. for lahars (Bartolini et al.,

101 2014; Sandri et al., 2014), landslides (Alexakis et al., 2014), earthquakes (Yazdani and Kowsari, 2017), pyroclastic flows  
102 (Bartolini et al., 2014; Sandri et al., 2014; Tierz et al., 2016), lava flows (Becerril et al., 2014; Favalli et al., 2009, 2012), tephra  
103 (Becerril et al., 2014; Bonadonna et al., 2005; Sandri et al., 2014)...). Such maps are produced by combining data on historical  
104 events with physical or statistical modelling (Calder et al., 2015). Surprisingly, no study is known to us that integrates  
105 information provided by probabilistic hazard maps in the assessment of impacts over an entire transport network.

106 To address this gap, this study proposes two metrics to characterize the importance of each segment in a road network in terms  
107 of accessibility to services in case a natural hazard occurs, using spatially explicit information on hazard probability. The first  
108 metric, the “road accessibility risk”, combines the road segment’s potential impact on the accessibility and travelling time of  
109 the population to the closest infrastructure (“road access vulnerability”) with the probability of occurrence of the hazard (“road  
110 hazard exposure”). The second metric, the “users’ path vulnerability”, considers, instead of the travelling time, the reliability  
111 of the alternative path the user needs to follow in case a road segment becomes disrupted or, in other words, the confidence  
112 that a user is not being impacted by the hazard when attempting to access the closest facility. We illustrate the use of the  
113 proposed metrics on Ngazidja Island (Union of the Comoros), a volcanic island where the road network is potentially exposed  
114 to lava flows. Access of the population to the closest hospital is used as an example of a key infrastructure that should be  
115 within reach, both in normal conditions as well as at the time of a hazardous event.

## 116 **2. Study area**

117 Located northwest of Madagascar, in the Mozambique Channel, Ngazidja is the most western island of the Comoros  
118 archipelago (Figure 1). It is exposed to a range of volcanic hazards, including lava flows. The central part of the island is  
119 formed by the active Karthala volcano (2361 m a.s.l.) which erupted every six to eight years on average over the last 200 years  
120 (Bachèlery et al., 2016). The roads on Ngazidja Island are classified into three categories (Figure 1): national, regional and  
121 local roads (PADDST, 2014). Historical lava flows (Bachèlery and Coudray, 1993) suggest that future volcanic impacts on  
122 the road network might be severe as the majority of lava flows in the past reached the coast line. The 1858 flow, for example,  
123 was issued at an altitude of 2100 m a.s.l. and travelled over a distance of 13 km to reach the ocean (Figure 1 ; Bachèlery and  
124 Coudray, 1993). During the 1977 eruption, an ‘a’ā lava flow issued from a fissure at 360 m a.s.l. on the southwest flank,  
125 crossed the villages of Singani and Hesta, and destroyed 566 meters of the road network (Krafft, 1982).

## 126 **3. Material and methods**

127 To assess the importance of road segments in people’s mobility to strategic infrastructure (i.e. hospitals) taking in account the  
128 probability of a road segment being affected by a hazard (i.e. lava flow), this research encompasses the following steps: (1)  
129 collecting data on population, strategic infrastructure and hazard probability, (2) building a digital representation of the road

130 network and assessing each road segment's attributes, (3) evaluating the population's accessibility to the closest infrastructure  
131 under normal and disrupted conditions and (4) calculating road accessibility risk and users' path vulnerability.

### 132 **3.1. Data collection**

#### 133 **3.1.1. Population data**

134 It is estimated that close to 302 000 people live on Ngazidja Island (estimate for 2013; Mossoux et al., 2018). The population  
135 estimated for each village is here used. While most of the population is concentrated in villages along the coastal area, 40% of  
136 the population lives in the capital Moroni and its surroundings (Figure 2).

#### 137 **3.1.2. Strategic infrastructure**

138 As key infrastructure, we consider six hospitals of the island providing specialized medical services (e.g. surgery, urgency,  
139 radiology...) (Centre d'Analyse et de Traitement de l'Information, 2016). Three of the six hospitals are located in the capital  
140 and its direct surroundings whereas the other three are located in secondary cities of the island: Mitsamouili, Mbéni and  
141 Foubouni (Figure 2). Due to a lack of data, the capacity and offered services of the hospitals are not considered in the  
142 analysis.

#### 143 **3.1.3. Lava flow hazard map**

144 A lava flow invasion hazard map identifies the locations that may be affected by a lava flow within a given time period (De  
145 La Cruz-Reyna et al., 2000; Sigurdsson et al., 2015; Thompson et al., 2017). The one used in this study provides for each  
146 location (corresponding with a cell of 90 m resolution) a probability of being inundated by lava flow during the next eruption  
147 (Figure 3). Probabilities have been computed using (1) QVAST, a plugin to produce a vent opening susceptibility map using  
148 information on the presence of volcanological structures (e.g. vents, fissures...) located on the volcano (Bartolini et al., 2013)  
149 and (2) Q-LavHA, an open-source plugin that simulates lava flow inundation probability from eruptive zones (e.g. vents,  
150 fissures and surfaces) on a Digital Elevation Model (DEM). Q-LavHA combines different models that determine the spatial  
151 propagation of a channelized 'a'ā lava and its terminal length using an iterative approach (Mossoux et al., 2016). It provides  
152 for each pixel a value between 0 and 1 which represents the pixel probability to be inundated during a next eruption. To produce  
153 lava flow hazard maps, Q-LavHA enables the user to consider vent opening susceptibility as calculated by QVAST and  
154 simulates lava flows from regularly distributed vents based on user defined input parameters that characterize the flow (Table  
155 1).

### 156 3.2. Building the road network and attributes

157 Because of the absence of detailed digital road network data, very high spatial resolution satellite images (Pléiades, 2013; 0.5  
158 m spatial resolution) and GPS tracks (Garmin eTrex 30x) acquired during three field missions (summer 2013, 2014 and 2016)  
159 have been used to delineate the road network (Figure 1). Pathways are not included in the network.

160 The digitized road segments were converted to a network formed by nodes and links. In this network nodes represent road  
161 intersections or the location of villages and infrastructure from which accessibility will be assessed. Each village is  
162 characterized by its number of inhabitants. Links in the network correspond to road segments and are described by (1) travel  
163 time to cross the segment and (2) cumulative susceptibility of the segment of being affected by lava flow.

164 To calculate travel time information on travel speed is required. Because no data on effective driving speed is available for the  
165 considered road network, the GPS tracks acquired during the three field missions were used to estimate the average speed  
166 reached on each road segment (km/h). A total of 139 GPS tracks were collected covering 93% of the national roads, 62% of  
167 the regional roads and 7% of the local roads. Some road segments are covered by several GPS tracks. As each individual road  
168 segment is assigned the average speed recorded by the overlaying tracks, a spatial variation within road segments of the same  
169 type can be observed. For segments not covered by GPS tracks, travel speed was estimated based on the average speed  
170 measured on road segments of the same type.

171 While the average speed reached on national road segments ( $speed_{\text{national roads}} = 27 \pm 10$  km/h) is higher compared to other road  
172 types, it is not much higher than on regional roads ( $speed_{\text{regional roads}} = 22 \pm 11$  km/h). Low speeds observed on national and  
173 regional roads are mostly related to the limited width and/or poor condition of the roads. The average speed on local road  
174 segments is limited to  $13 \pm 11$  km/h due to the sinuosity and the location of these segments within cities and villages.  
175 Measurements are of course dependent on driver characteristics, mode of transport (e.g. personal car, taxi or public bus), time  
176 of the day and moment of the year, as well as the state of the road at the time of the acquisition. No differentiation between  
177 different modes of transport was possible. Despite these biases, the GPS measurements give a realistic impression of the local  
178 transport characteristics and are representative of the spatial variability of effective transport velocity on the road network.  
179 These data (in km/h) were used to estimate the travel time (in seconds) over each road segment  $i$  (Equation 1):

$$180 \text{ Travel time}_i = \frac{\text{Length}_i}{\text{Speed}_i * \left(\frac{1000}{3600}\right)} \quad (1)$$

181 Each road segment was finally characterized by its susceptibility of being inundated, and therefore blocked, by a lava flow.  
182 To calculate this susceptibility, the probabilities of the lava flow hazard map cells (Figure 3) underlying all road segments  
183 were normalized to sum to one. Then for each road segment  $i$  these normalized values were summed up to produce a relative  
184 measure of the susceptibility of the segment to be affected by a lava flow ( $h_i$ ). A sum of the normalised probabilities is here  
185 favored, instead of calculating an average of the original probability values for each segment because this way the length of  
186 the segment is accounted for. Indeed, all other things being equal, the longer the road segment, the higher the chance will be  
187 that it could be blocked due to a lava flow.

188 **3.3. Accessibility before and after disruption**

189 Considering an undisturbed road network, each village weighted by its number of inhabitants (Mossoux et al., 2018) was, in  
190 first instance, assigned to the closest infrastructure based on Dijkstra's shortest path algorithm (Dijkstra, 1959) (Figure 4 -  
191 normal situation). The shortest path was calculated according to travel time (s).

192 In a second stage, each road segment was iteratively removed from the network to simulate the effect of a road segment being  
193 obstructed (Appert and Chapelon, 2007). Based on the network with one segment removed, Dijkstra's shortest path algorithm  
194 was applied again to define the new shortest path to the closest infrastructure from each village (Figure 4 - disrupted situation).  
195 Comparison with the undisturbed road network allows defining the overall impact of the road segment closure on the  
196 accessibility of the population to the closest infrastructure. Three scenarios are possible:

- 197 - Inhabitants of a village are unaffected by the road removal. The closest infrastructure and the travel time are still the  
198 same as in the undisturbed situation.
- 199 - Inhabitants of a village are affected ( $pop_{affected}$ ). The road removal increases the journey in time or assigns the road  
200 users to a new infrastructure which is located further away.
- 201 - Inhabitants of a village become isolated from available services and remain unserved ( $pop_{unserved}$ ). They no longer  
202 have access to any of the present service infrastructures (Jenelius et al., 2006).

203 At the end of the process, each road segment is characterized by the total number of people it would affect or isolate if the road  
204 segment would become obstructed (Figure 4). Additionally, the travel time (s) and the hazard exposure experienced by the  
205 affected population before and after the road segment obstruction is recorded and used to define a journey and reliability ratio  
206 specific for each affected user. The first ratio defines the travel time change experienced by the users (Figure 4). The higher  
207 the journey ratio, the higher the users' relative increase in travelling time after the disruption. The second ratio assesses the  
208 difference of the users' path exposure to the hazard (

209 Figure 4 - Accessibility assessment before and after a disruption using Dijkstra's shortest path algorithm. People affected and  
210 unserved are weighted by the Journey Ratio which assesses the travel time increase caused by the disruption and re-routing.

211 Figure 5). When users access an infrastructure using the shortest path, they use road segments having a susceptibility to be  
212 affected by the hazard ( $h_i$ ). The sum of the road segments' susceptibility for all segments taken by users to access the closest  
213 facility ( $H_i$ ) is considered in this study as being representative of the users' path reliability. It therefore represents the  
214 confidence that a user is not being impacted by the hazard when following the shortest path to access the closest facility

215 (Immers et al., 2004; Jenelius et al., 2006). Comparison of the users' path exposure before and after the disruption enables to  
 216 define a reliability ratio. The lower the ratio, the safer the path taken by the users relative to the original path.

### 217 3.4. The metrics

#### 218 3.4.1. Road accessibility risk

219 The road accessibility risk ( $Risk_i$ ) combines road access vulnerability ( $V_i$ ) with the road segment's susceptibility to be affected  
 220 by the hazard ( $h_i$ ):

$$221 Risk_i = V_i * h_i \quad (2)$$

222 The road access vulnerability index ( $V_i$ ) summarizes the impact of a road segment's obstruction on the population's  
 223 accessibility to the closest infrastructure (Equation 3). Population that will be affected by a rerouting ( $pop_{affected}$ ) and  
 224 population completely disconnected from access to services ( $pop_{unserved}$ ) are both integrated into the index. The  $pop_{j,affected}$   
 225 is weighted based on the *Journey Ratio<sub>j</sub>* (Equation 4, see also Figure 4), which represents for each village ( $j$ ) the journey  
 226 difference in time (s) before ( $t_{j,normal}$ ) and after ( $t_{j,disturbed}$ ) the road segment obstruction. The journey ratio varies between  
 227 0 and 1 representing none to large changes in the journey, respectively. The  $pop_{unserved}$  is weighted by one as this is the worse  
 228 case scenario. The vulnerability index ( $V_i$ ) varies from 0, for road segments with no impact on people's accessibility, to a  
 229 maximum of 1. In this last situation, the entire population of the island would have no access to services through the obstruction  
 230 of the segment, which in practice can only occur if service supply would be restricted to one location that is completely cut off  
 231 from the road network.

$$232 V_i = \frac{\sum_{j=1}^n (pop_{j,affected} * Journey Ratio_j) + pop_{j,unserved}}{pop_{total}} \quad (3)$$

$$233 Journey Ratio_j = \frac{t_{j,disturbed} - t_{j,normal}}{t_{j,disturbed}} \quad (4)$$

234 where  $n$  represents the total number of villages in the study area.

235 Knowing the road access vulnerability ( $V_i$ ) for each segment, it is then combined with the road segment's susceptibility to be  
 236 affected by the hazard ( $h_i$ ) (see section 3.2) to obtain the road accessibility risk ( $Risk_i$ ) caused by the obstruction of road  
 237 segment  $i$  according to Eq. 2.

#### 238 3.4.2. Users' path vulnerability

239 Similarly to the road access vulnerability index, the users' path vulnerability metric ( $V_{u,i}$ ) integrates the population affected by  
 240 a rerouting ( $pop_{affected}$ ) and the population completely disconnected ( $pop_{unserved}$ ). But instead of weighting the  $pop_{affected}$   
 241 based on the journey travelling time difference, the affected population is weighted by the *Reliability Ratio<sub>j</sub>* (Equation 5).

242 Considering the user's path exposure as being the sum of susceptibility values for all segments crossed by a user during his  
 243 journey to the closest service ( $H_i$ ), this ratio records changes in the users' path exposure to the hazard before and after road  
 244 segment obstruction (Equation 6). The *Reliability Ratio<sub>j</sub>* varies between -1 and 1 as the alternative path, which users are  
 245 forced to take, may consist of road segments with an overall lower or higher exposure ( $H_{j,disturbed}$ ) to the hazard compared to  
 246 the original path ( $H_{j,normal}$ ). If the alternative road improves the path's reliability, i.e. the user is forced to take a path with a  
 247 lower chance of being impacted by the hazard, the ratio will be negative. The ratio will be equal to zero if the users' path  
 248 reliability remains unchanged before and after the segment interruption. In case the hazard susceptibility of the alternative path  
 249 is higher than in the normal situation, the ratio is positive. Again, the  $pop_{unserved}$  is weighted by one as this corresponds to the  
 250 worst-case scenario. The users' path vulnerability ( $V_{u,i}$ ) similarly varies between -1 and 1.

$$251 \quad V_{u,i} = \frac{\sum_{j=1}^n (pop_{j,affected} * Reliability\ Ratio_j) + pop_{j,unserved}}{pop_{total}} \quad (5)$$

$$252 \quad Reliability\ Ratio_j = \frac{H_{j,disturbed} - H_{j,normal}}{H_{j,disturbed} + H_{j,normal}} \quad (6)$$

### 253 **3.5. Modelling assumptions**

254 Accessibility assessment is a process that is computationally demanding (Postance et al., 2017). The number of alternative  
 255 paths increases with the size of the road network, the number of villages and the number of infrastructures to process. While  
 256 integrating travellers' demand (in this case access to the closest hospital) into the road segment analysis already leads to a  
 257 more realistic representation of accessibility (Jenelius and Mattsson, 2015; Taylor and Susilawati, 2012), the following  
 258 assumptions have been made in this study to make the computation feasible:

- 259 - The disruption affects only one segment at a time and is considered to last long enough. People will therefore not  
 260 postpone their departure and will adapt to the situation by using alternative roads to access the closest infrastructure  
 261 (Jenelius and Mattsson, 2015).
- 262 - Time is the only element influencing their decision to access an infrastructure.
- 263 - Users have a perfect knowledge of the network and know which is the shortest alternative if an alternative exists  
 264 (Jenelius and Mattsson, 2015).
- 265 - All roads can be used in either direction.
- 266 - The travel demand is constant at any time of the day and at any moment of the year, even during a disruption (Jenelius  
 267 and Mattsson, 2015). At the time of the disruption, all inhabitants are residing in their home village. The hazard does  
 268 not cause fatalities that will affect the travel demand.
- 269 - The disruption induces no congestion (Jenelius and Mattsson, 2015) which is a reasonable assumption for Ngazidja  
 270 Island where the vehicle fleet is limited outside the capital.
- 271 - The road network capacity is adapted to the travel demand.

272 **4. Results**

273 **4.1. Road accessibility risk**

274 **4.1.1. Road access vulnerability**

275 In the context of Ngazidja Island, the road access vulnerability ( $V_i$ ) analysis highlights that the most vulnerable roads are  
276 located in the close surrounding of the hospital facilities (

277 Figure 4 - Accessibility assessment before and after a disruption using Dijkstra's shortest path algorithm. People affected and  
278 unserved are weighted by the Journey Ratio which assesses the travel time increase caused by the disruption and re-routing.

279 Figure 5 - Accessibility assessment before and after a disruption using Dijkstra's shortest path algorithm. People affected and  
280 unserved are weighted by the Reliability Ratio which assesses how users' path exposure changes when taking the alternative  
281 shortest path in time to access the infrastructure.

282 Figure 6). Since close to facilities the number of travellers using these segments is important (

283 Figure 4 - Accessibility assessment before and after a disruption using Dijkstra's shortest path algorithm. People affected and  
284 unserved are weighted by the Journey Ratio which assesses the travel time increase caused by the disruption and re-routing.

285 Figure 5 - Accessibility assessment before and after a disruption using Dijkstra's shortest path algorithm. People affected and  
286 unserved are weighted by the Reliability Ratio which assesses how users' path exposure changes when taking the alternative  
287 shortest path in time to access the infrastructure.

288 Figure 6a), closure of a road segment close to the hospital will have a large impact on accessibility for a large part of the  
289 population. Road segments with limited road alternatives (

290 Figure 4 - Accessibility assessment before and after a disruption using Dijkstra's shortest path algorithm. People affected and  
291 unserved are weighted by the Journey Ratio which assesses the travel time increase caused by the disruption and re-routing.

292 Figure 5 - Accessibility assessment before and after a disruption using Dijkstra's shortest path algorithm. People affected and  
293 unserved are weighted by the Reliability Ratio which assesses how users' path exposure changes when taking the alternative  
294 shortest path in time to access the infrastructure.

295 Figure 6b) and the first segment of dead-end roads (

296 Figure 4 - Accessibility assessment before and after a disruption using Dijkstra's shortest path algorithm. People affected and  
297 unserved are weighted by the Journey Ratio which assesses the travel time increase caused by the disruption and re-routing.

298 Figure 5 - Accessibility assessment before and after a disruption using Dijkstra's shortest path algorithm. People affected and  
299 unserved are weighted by the Reliability Ratio which assesses how users' path exposure changes when taking the alternative  
300 shortest path in time to access the infrastructure.

301 Figure 6c) are also characterized by higher road access vulnerability. When road redundancy is limited, the users' travelling  
302 time inevitably increases as it forces users to take a longer alternative route. Dead-end roads represent the only connection of  
303 villages to the network. Their closure directly induces that the whole population of a village loses its road access to the hospital  
304 ( $pop_{\text{unserved}}$ ). Idjikoundzi and Maouéni, for example, are two villages located high up on the volcano flank. Both villages depend  
305 on a single road segment to reach key infrastructure (

306 Figure 4 - Accessibility assessment before and after a disruption using Dijkstra's shortest path algorithm. People affected and  
307 unserved are weighted by the Journey Ratio which assesses the travel time increase caused by the disruption and re-routing.  
308 Figure 5 - Accessibility assessment before and after a disruption using Dijkstra's shortest path algorithm. People affected and  
309 unserved are weighted by the Reliability Ratio which assesses how users' path exposure changes when taking the alternative  
310 shortest path in time to access the infrastructure.

311 Figure 6c). If this segment would become obstructed by a lava flow, it would prevent evacuation to hospitals or direct provision  
312 of emergency help to these villagers.

#### 313 **4.1.2. Road hazard exposure**

314 Figure 7 shows the susceptibility of each road segment of being affected by lava flow ( $h_i$ ) calculated as the sum of normalized  
315 hazard probability values occurring along the segment. The road segments characterized by the highest susceptibility are  
316 located on the northern flank of the Karthala massive and in the south. It concerns roads at higher elevation close to the volcanic  
317 rift zones along which most eruptions are initiated. Road segments located in the region of the 1977 eruption, near Singani and  
318 Hetsa villages, also present high chances of being affected by lava flow. Even if the probability for lava to outflow from "la  
319 Porte d'Itsandra" and overflow the downstream areas is high (Figure 3), the probability decreases with distance. The probability  
320 that such flows reach road segments in the capital city Moroni is rather small. Because the hazard exposure for each segment,  
321 referred to as susceptibility here, is defined by summing up the normalized probability values of all pixels underlying the road  
322 segment, exposure of a segment to hazard is influenced both by probability values at pixel level as well as by the length of the  
323 segment. This reflects the fact that longer segments having a chance of being affected by lava flows at different locations along  
324 the segment are also more exposed to lava flow hazard and thus have a higher chance of being blocked by one or more lava  
325 flows. Accordingly, shorter segments as observed in the capital and in most villages (e.g. Koimbani - Figure 7) will have lower  
326 susceptibility values than some longer segments, even if the area is highly exposed.

#### 327 **4.1.3. Road accessibility risk**

328 Multiplying road access vulnerability for each segment ( $V_i$ ) with the susceptibility of the road segment of being affected by a  
329 lava flow ( $h_i$ ) enables identifying the accessibility risk associated with each road segment (Figure 8). Road segments with a  
330 high accessibility risk are segments with a limited number of alternative roads (road redundancy) in the immediate

331 surroundings (Figure 8a), first segments of dead-end roads (Figure 8b), and roads associated with a high lava flow susceptibility  
332 (Figure 8c).

#### 333 **4.2. Users' path vulnerability**

334 Integrating users' exposure to hazard while travelling to the closest facility enables to identify whether the alternative shortest  
335 path in case of a road segment obstruction increases or decreases hazard exposure. The former results in an increase in users'  
336 path vulnerability, the latter in a decrease. Main road segments located close to and within the area potentially affected by  
337 Karthala lava flows show high users' path vulnerability index values ( $V_{u,i}$ ) (Figure 9a-b-c) since closure of these road segments  
338 would induce some users to choose for a less reliable route. Moreover, it is also interesting to note that the users' path  
339 vulnerability of some road segments is negative (Figure 9d). This indicates that the alternative shortest path taken by most  
340 users that would normally be traversing this road segment is associated with a lower probability to be interrupted by lava flow,  
341 and that the reliability of the route for these users therefore improves.

#### 342 **5. Discussion**

343 The metrics proposed in this study provide a good overview of which road segments are the most strategic in a road network  
344 in terms of impact of road closure on access to key infrastructure in case a hazard occurs.

345 For long term management, the road accessibility risk metric (1) identifies road segments that are exposed to hazard and that  
346 would substantially reduce access to infrastructure if being obstructed by a lava flow and (2) enables to quickly calculate and  
347 visualize the impact of any changes proposed in the road network (e.g. in the network's structure or the segment's  
348 characteristics) on accessibility and exposure. Such impacts must be carefully interpreted and discussed since modifications  
349 of the road network have a cost and even if the risk in some parts of the region may be reduced, it can be at the expense of a  
350 higher risk in other locations.

351 To lower the risk associated with each road segment, measures can be taken to prevent or reduce the impact of specific hazards  
352 (e.g. rock safety net, drainage channel, dykes). Engineering works can also make the roads more hazard-proof or reduce the  
353 hazard's direct physical impact. In the case of lava flows, however, little can be done to prevent the hazard or to adapt road  
354 infrastructure to better cope with the hazard. Measures should therefore focus on reducing the impact of road obstruction on  
355 the population's accessibility. Modifying the population demand on the network can, for example, reduce road access  
356 vulnerability associated with particular road segments. For the current situation, the overall road access vulnerability index  
357 associated with the road network within the service area of the Foubouni hospital, for example, is equal to 4.99 (Figure 10a).  
358 As it can be observed in Figure 10b, the construction of a new road segment has a positive impact on the overall road access  
359 vulnerability associated with the road network in the service area. People which were before isolated or highly impacted due  
360 to a road obstruction now have an alternative path to the hospital. Redundancy positively influences road access vulnerability  
361 (Mattsson and Jenelius, 2015; Taylor et al., 2006) and lowers the overall road access vulnerability index to 4.45. The

362 development of new infrastructure can also positively influence road access vulnerability (Figure 10c). A new hospital location  
363 within the service area of Foubouni hospital reduces overall road access vulnerability within the area to 4.09.

364 Improvement of the speed can finally also contribute to changes in road access vulnerability. Suppose that the average speed  
365 of  $27 \pm 10$  km/h reached on national roads is improved to 70 km/h through increased road width, better road conditions and  
366 maintenance. The proposed methodology then allows a quick evaluation of the impact on road access vulnerability. While  
367 increasing the speed does not allow reducing the overall road access vulnerability it tends to concentrate traffic flow on the  
368 fastest road segments (Figure 11) (Taylor et al., 2006). Alternatively, road segments least exposed to hazard could be  
369 preferentially improved to increase the effective speed on these roads. This would re-direct users to these more rapid roads and  
370 decrease the risk of users being impacted by a road obstruction due to a hazard.

371 The second metric presented in this research, the users' path vulnerability metric, defines the impact the closure of a road  
372 segment would have on the reliability of the alternative route in terms of exposure to hazard. This metric can be used for short  
373 term management as it identifies the road segments increasing or lowering the exposure of users to the hazard when travelling  
374 to the closest infrastructure. It can be used as an argument to:

- 375 - Keep some road segments open: close to the border of the area that is potentially affected by Karthala lava flows,  
376 road segments have high users' path vulnerability index values (Figure 9a-b). Closure of these road segments would  
377 induce some users to have to choose for a less reliable route. Indeed, if these road segments become obstructed, people  
378 will be forced to take an alternative route, principally more to the south, which is more exposed to lava flow hazard  
379 (Figure 3).
- 380 - Prioritize repair of obstructed road segments: road segments within the area that is potentially affected by Karthala  
381 lava flows and that are associated with a high users' path vulnerability index (Figure 9c) may be prioritized for repair  
382 if obstructed at the same time as other segments, if the modelling shows that their obstruction would force people to  
383 expose themselves to a higher hazard probability when taking the detour route.
- 384 - Preventively close some road sections: road segments with a negative users' path vulnerability may be closed in case  
385 an event is expected in the service area containing the road segment, in order to re-orientate the flow of users to less  
386 exposed roads (Figure 9d).

## 387 **6. Perspectives**

388 Modelling of accessibility in case of a hazard, as proposed in this study, assumes that the disruption of the road network affects  
389 only one segment at a time. Future improvements of the model should be able to deal with obstruction of multiple segments,  
390 as lava flows can affect different road segments while following their path or develop branches in different directions. Attention  
391 should also be given to a proper representation of the road network and its attributes, as in other potential study areas road  
392 networks can be more complex than on Ngazidja Island (e.g. one direction roads, turn restrictions, overpasses, tunnels...).

393 For the sake of illustration, accessibility to only one type of service (i.e. hospital) was discussed, without taking in account  
394 functional characteristics or capacity constraints. It would be interesting to generalize the proposed methodology to be able to  
395 concurrently cope with different types of services (e.g. emergency services, economic activity...) and to integrate the capacity  
396 and attractiveness of specific infrastructures using a gravity modelling approach (Guagliardo, 2004; Luo and Qi, 2009). As  
397 such, other characteristics governing the choice of infrastructure can be incorporated in the analysis.  
398 One should also keep in mind that in our analysis travel demand is assumed constant at any time of the day, week, and at any  
399 moment of the year, and during a disruption, and that no congestion effects are taken in account. Taking diurnal, weekly and  
400 seasonal differences in travel demand and movement patterns in account would require detailed information about human  
401 activity patterns and travel behaviour, which was not available for this study. However, with the rise of big data on resident's  
402 mobility patterns one may expect that more realistic scenario analysis of impacts of road obstruction on accessibility will  
403 become feasible, also in the case of a hazard. Implementation of these modelling perspectives would contribute to a more  
404 realistic simulation of road segments' importance and users' behaviour on the road network.  
405 Finally, the analysis presented in this research focuses on lava flow hazard only. Yet other hazards may be capable of blocking  
406 a road as well (e.g. ash fall, floods, rock fall...). Lava flows are natural hazards that have a high destructive power on  
407 infrastructure. When a lava flow hits a road, it is realistic to assume that the road is completely obstructed. But this is not  
408 always the case with other natural hazards. In these situations, when a road is affected, users might be able to still use the road  
409 segment. Based on the type and intensity of the hazard, the users' travel time will be affected to some extent. Speed disruption  
410 functions or functional losses described in other studies (Jenkins et al., 2015; Pregolato et al., 2017; Wilson et al., 2012) might  
411 be integrated in the shortest path analysis and therefore enable adapting the proposed methodology to a wider range of hazards  
412 (e.g. ash fall, congestion...).

## 413 **7. Conclusions**

414 Accessibility analysis in a hazardous situation is important since the population must be able to effectively evacuate, access  
415 shelters or medical infrastructure, while emergency services must be able to assist the population in situ. For hazards with a  
416 spatially heterogeneous probability of occurrence, combining hazard maps with road network accessibility measures provides  
417 a new way to support functional risk assessment.

418 The current study presents two metrics to assess the importance of a road segment on people's mobility effectively using  
419 location specific information provided by probabilistic hazard maps. Both metrics enable quantitative assessment of impacts  
420 of hazard on accessibility to critical infrastructure and result in maps that may support and feed discussions about the  
421 development of new infrastructure, road capacity increase, maintenance and emergency procedures.

422 The road accessibility risk metric proposed in this study assesses the impact of each road segment's obstruction on the  
423 population's accessibility to infrastructure and combines it with the road segment's susceptibility of being affected by a hazard.

424 The users' path vulnerability metric defines the impact the closure of a road segment has on the reliability of the alternative

425 route a user of the road network would be forced to take. The metric highlights that not only roads in a hazardous environment  
426 must be considered in risk assessment, also road segments located further away from the hazard may be important as their  
427 obstruction may force people to take an alternative road which is less reliable. User's path vulnerability may also be used to  
428 prioritize the re-opening of affected segments or to preventively close some road segments located in the proximity of an  
429 expected hazard to re-orientate users to less exposed roads. The two metrics presented in this study may contribute to a rational  
430 analysis of accessibility related risks of natural hazards and scenario analysis for reducing these risks.

431 **8. Code and data availability**

432 Python codes developed in this study and GIS datasets specifically developed for this study are available upon request to the  
433 authors.

434 **9. Authors' contribution**

435 SM designed the research, conducted the analysis and wrote the manuscript. MK and FC advised on the study design,  
436 supervised the research and revised the manuscript.

437 **10. Competing interests**

438 The authors declare that they have no conflict of interest.

439 **11. Acknowledgments**

440 We are extremely grateful to the “Centre National de Documentation et de Recherche Scientifique”, for its technical support  
441 during the three missions done on Ngazidja Island. Many thanks to Hamid Soulé and Shafik Bafakih for their assistance, and  
442 for sharing their expertise during these missions. The authors also would like to thank Marc Van Molle and the “Fonds  
443 Wetenschappelijk Onderzoek”, for their financial support. Thank you to all Comorian institutions for sharing information with  
444 us making this research possible. We thank two anonymous reviewers and the responsible editor for their comments that helped  
445 to improve the manuscript.  
446

447 **12. References**

- 448 Alexakis, D. D., Agapiou, A., Tzouvaras, M., Themistocleous, K., Neocleous, K., Michaelides, S. and Hadjimitsis, D. G.:  
449 Integrated use of GIS and remote sensing for monitoring landslides in transportation pavements: The case study of Paphos  
450 area in Cyprus, *Nat. Hazards*, 72(1), 119–141, doi:10.1007/s11069-013-0770-3, 2014.
- 451 Appert, M. and Chapelon, L.: Measuring urban road network vulnerability using graph theory: The case of Montpellier’s road  
452 network, *La mise en Cart. des risques Nat.*, 1–22, 2007.
- 453 Bachèlery, P. and Coudray, J.: Carte Géologique des Comores: Notice explicative de la carte volcano-tectonique de la Grande  
454 Comore (Ngazidja), Ministère., edited by Ministère Français de la Coopération., 1993.
- 455 Bachèlery, P., Lénat, J.-F., Di Muro, A. and Michon, L.: Active volcanoes of the southwest Indian ocean Piton de la Fournaise  
456 and Karthala, *Active vol.*, Springer., 2016.
- 457 Bartolini, S., Cappello, A., Martí, J. and Del Negro, C.: QVAST: A new Quantum GIS plugin for estimating volcanic  
458 susceptibility, *Nat. Hazards Earth Syst. Sci.*, 13(11), 3031–3042, doi:10.5194/nhess-13-3031-2013, 2013.
- 459 Bartolini, S., Geyer, A., Martí, J., Pedrazzi, D. and Aguirre-Díaz, G.: Volcanic hazard on Deception Island (South Shetland  
460 Islands, Antarctica), *J. Volcanol. Geotherm. Res.*, 285, 150–168, doi:10.1016/J.JVOLGEORES.2014.08.009, 2014.
- 461 Becerril, L., Bartolini, S., Sobradelo, R., Martí, J., Morales, J. M. and Galindo, I.: Long-term volcanic hazard assessment on  
462 El Hierro (Canary Islands), *Nat. Hazards Earth Syst. Sci.*, 14, 1853–1870, doi:10.5194/nhess-14-1853-2014, 2014.
- 463 Bil, M., Sedonik, J., Kubecek, J., Vodak, R. and Bilova, M.: Road Network Segments At Risk – Vulnerability Analysis and  
464 Natural Hazards Assessment, *Sci. Popul. Prot.*, 1–18 [online] Available from: [http://www.population-](http://www.population-protection.eu/prilohy/casopis/eng/20/87.pdf)  
465 [protection.eu/prilohy/casopis/eng/20/87.pdf](http://www.population-protection.eu/prilohy/casopis/eng/20/87.pdf), 2014.
- 466 Blake, D. M., Deligne, N. I., Wilson, T. M., Lindsay, J. M. and Woods, R.: Investigating the consequences of urban volcanism  
467 using a scenario approach II: Insights into transportation network damage and functionality, *J. Volcanol. Geotherm. Res.*, 340,  
468 92–116, doi:10.1016/j.jvolgeores.2017.04.010, 2017.
- 469 Bonadonna, C., Connor, C. B., Houghton, B. F., Connor, L., Byrne, M., Laing, A. and Hincks, T. K.: Probabilistic modeling  
470 of tephra dispersal: Hazard assessment of a multiphase rhyolitic eruption at Tarawera, New Zealand, *J. Geophys. Res. Solid*  
471 *Earth*, 110(3), 1–21, doi:10.1029/2003JB002896, 2005.
- 472 Calder, E. S., Wagner, K. and Ogburn, S. E.: Volcanic hazard maps, in *Global volcanic hazards and risk*, edited by S. Loughlin,  
473 S. Sparks, S. Brown, S. Jenkins, and C. Vye-Brown, pp. 335–342, Cambridge University Press., 2015.
- 474 Centre d’Analyse et de Traitement de l’Information: Données spatiales - Comores, 2016.
- 475 Chang, S. E. and Nojima, N.: Measuring post-disaster transportation system performance: The 1995 Kobe earthquake in  
476 comparative perspective, *Transp. Res. Part A Policy Pract.*, 35(6), 475–494, doi:10.1016/S0965-8564(00)00003-3, 2001.
- 477 Dijkstra, E. W.: A Note on Two Problems in Connexion with Graphs, *Numer. Math.*, 271(1), 269–271, 1959.
- 478 Favalli, M., Chirico, G. D., Papale, P., Pareschi, M. T. and Boschi, E.: Lava flow hazard at Nyiragongo volcano, D.R.C. 1.  
479 Model calibration and hazard mapping, *Bull. Volcanol.*, 71(4), 363–374, doi:10.1007/s00445-008-0233-y, 2009.

480 Favalli, M., Tarquini, S., Papale, P., Fornaciari, A. and Boschi, E.: Lava flow hazard and risk at Mt. Cameroon volcano, *Bull.*  
481 *Volcanol.*, 74(2), 423–439, doi:10.1007/s00445-011-0540-6, 2012.

482 Hong, L., Ouyang, M., Peeta, S., He, X. and Yan, Y.: Vulnerability assessment and mitigation for the Chinese railway system  
483 under floods, *Reliab. Eng. Syst. Saf.*, 137, 58–68, doi:10.1016/J.RESS.2014.12.013, 2015.

484 Immers, B., Yperman, I., Stada, J. and Bleukx, A.: Reliability and robustness: Problem survey., 2004.

485 Institute of Electrical and Electronics Engineers: IEEE standard computer dictionary: A compilation of IEEE standard  
486 computer glossaries, New York., 1990.

487 Jenelius, E. and Mattsson, L.-G.: Road network vulnerability analysis: Conceptualization, implementation and application, ,  
488 doi:10.1016/j.compenvurbsys.2014.02.003, 2015.

489 Jenelius, E., Petersen, T. and Ran Mattsson, L.-G.: Importance and exposure in road network vulnerability analysis, *Transp.*  
490 *Res. Part A*, 40, 537–560, doi:10.1016/j.tra.2005.11.003, 2006.

491 Krafft, M.: L'éruption volcanique du Karthala en avril 1977, 1982.

492 De La Cruz-Reyna, S., Meli, R. and Quaas, R.: Volcanic crises management, in *The Encyclopedia of Volcanoes*, edited by H.  
493 Sigurdsson, B. Houghton, S. R. McNutt, H. Rymer, and J. Stix, pp. 1199–1214, Academic Press, USA., 2000.

494 Mattsson, L.-G. and Jenelius, E.: Vulnerability and resilience of transport systems - A discussion of recent research, *Transp.*  
495 *Res. Part A*, 81, 16–34, doi:10.1016/j.tra.2015.06.002, 2015.

496 Mossoux, S., Kervyn, M., Soulé, H. and Canters, F.: Mapping population distribution from high resolution sensed imagery in  
497 a data poor setting, *Remote Sens.*, (2015), 1–21, 2018.

498 Mossoux, Saey, M., Bartolini, S., Poppe, S., Canters, F. and Kervyn, M.: Q-LAVHA: A flexible GIS plugin to simulate lava  
499 flows, *Comput. Geosci.*, 97, 98–109, doi:10.1016/j.cageo.2016.09.003, 2016.

500 Nagurney, A. and Qiang, Q.: Fragile networks: Identifying vulnerabilities and synergies in an uncertain age, *Int. Trans. Oper.*  
501 *Res.*, 19, 123–160, 2012.

502 PADDST: Type de route à Ngazidja, 2014.

503 Peeta, S., Sibel Salman, F., Gunec, D. and Viswanath, K.: Pre-disaster investment decisions for strengthening a highway  
504 network, *Comput. Oper. Res.*, 37(10), 1708–1719, doi:10.1016/J.COR.2009.12.006, 2010.

505 Postance, B., Hillier, J., Dijkstra, T. and Dixon, N.: Extending natural hazard impacts: An assessment of landslide disruptions  
506 on a national road transportation network, *Environ. Res. Lett.*, 12(1), doi:10.1088/1748-9326/aa5555, 2017.

507 Pregnolato, M., Ford, A., Wilkinson, S. M. and Dawson, R. J.: The impact of flooding on road transport: A depth-disruption  
508 function, *Transp. Res. Part D Transp. Environ.*, 55, 67–81, doi:10.1016/j.trd.2017.06.020, 2017.

509 Sandri, L., Thouret, J. C., Constantinescu, R., Biass, S. and Tonini, R.: Long-term multi-hazard assessment for El Misti volcano  
510 (Peru), *Bull. Volcanol.*, 76(2), 1–26, doi:10.1007/s00445-013-0771-9, 2014.

511 Sigurdsson, H., Houghton, B., McNutt, S. R., Rymer, H. and Stix, J.: *The encyclopedia of volcanoes*, Academic P., John  
512 Fedor., 2015.

513 Sohn, J.: Evaluating the significance of highway network links under the flood damage: an accessibility approach, *Transp.*

514 Res. Part A Policy Pract., 40(6), 491–506, doi:10.1016/J.TRA.2005.08.006, 2006.

515 Sullivan, J. L., Novak, D. C., Aultman-Hall, L. and Scott, D. M.: Identifying critical road segments and measuring system-  
516 wide robustness in transportation networks with isolating links: A link-based capacity-reduction approach, *Transp. Res. Part*  
517 *A*, 44, 323–336, doi:10.1016/j.tra.2010.02.003, 2010.

518 Taylor, M. A. P., Sekhar, S. V. C. and D’Este, G. M.: Application of accessibility based methods for vulnerability analysis of  
519 strategic road networks, *Networks Spat. Econ.*, 6(3–4), 267–291, doi:10.1007/s11067-006-9284-9, 2006.

520 Taylor, M. A. P. and Susilawati: Remoteness and accessibility in the vulnerability analysis of regional road networks, *Transp.*  
521 *Res. Part A Policy Pract.*, 46(5), 761–771, doi:10.1016/j.tra.2012.02.008, 2012.

522 Thompson, M. A., Lindsay, J. M. and Leonard, G. S.: More than meets the eye: Volcanic hazard map design and visual  
523 communication, *Adv. Volcanol.*, 1–14, doi:10.1007/11157\_2016\_47, 2017.

524 Tierz, P., Sandri, L., Costa, A., Zaccarelli, L., Di Vito, M. A., Sulpizio, R. and Marzocchi, W.: Suitability of energy cone for  
525 probabilistic volcanic hazard assessment: Validation tests at Somma-Vesuvius and Campi Flegrei (Italy), *Bull. Volcanol.*,  
526 78(11), doi:10.1007/s00445-016-1073-9, 2016.

527 Winter, M. G., Shearer, B., Palmer, D., Peeling, D., Harmer, C. and Sharpe, J.: The economic impact of landslides and floods  
528 on the road network, *Procedia Eng.*, 143, 1425–1434, doi:10.1016/J.PROENG.2016.06.168, 2016.

529 Yazdani, A. and Kowsari, M.: A probabilistic procedure for scenario-based seismic hazard maps of Greater Tehran, *Eng.*  
530 *Geol.*, 218, 162–172, doi:10.1016/J.ENGGEOL.2017.01.013, 2017.

531

532 **13. Figure Captions**

533 Figure 1 - Road network (own processing) on Ngazidja Island and some historical lava flows. The insets show the location of  
534 the island in Africa and within the Comorian archipelago.

535 Figure 2 - Population repartition estimated for 2013 (Mossoux et al., 2018) and location of the hospitals (Centre d'Analyse et  
536 de Traitement de l'Information, 2016) considered in the road accessibility risk and users' path vulnerability assessment.

537 Figure 3 - Lava flow hazard probability map of Karthala volcano (own processing). The inset provides a closer view on the  
538 caldera and the "Porte d'Itsandra" which is an opening in the North of the caldera where lava can escape.

539 Figure 4 - Accessibility assessment before and after a disruption using Dijkstra's shortest path algorithm. People affected and  
540 unserved are weighted by the Journey Ratio which assesses the travel time increase caused by the disruption and re-routing.

541 Figure 5 - Accessibility assessment before and after a disruption using Dijkstra's shortest path algorithm. People affected and  
542 unserved are weighted by the Reliability Ratio which assesses how users' path exposure changes when taking the alternative  
543 shortest path in time to access the infrastructure.

544 Figure 6 - Road access vulnerability map representing the impact of each road segment obstruction on the population's  
545 accessibility to the closest infrastructure in terms of travel time.

546 Figure 7 - Road hazard exposure map for the Karthala volcano showing susceptibility to lava flow hazard for each road segment  
547 with an inset on Koimbani. The upper inset represents the lava flow hazard probability map in the surrounding of Koimbani.  
548 Roads are overlaid on top of the hazard map. The lower inset shows susceptibility values for road segments in Koimbani.

549 Figure 8 - Accessibility risk map for road segments combining road access vulnerability based on travel time (s) to the closest  
550 infrastructure with road segment susceptibility to Karthala lava flows.

551 Figure 9 - Road users' path vulnerability.

552 Figure 10 - Modification of the actual road access vulnerability (a) by constructing a new road segment (b) or by developing  
553 a new infrastructure (c). The overall road access vulnerability is the sum of the road access vulnerability values of all road  
554 segments within the Foubouni hospital service area.

555 Figure 11 - Impact on road access vulnerability of an improvement of the speed that can be reached on national roads.

556

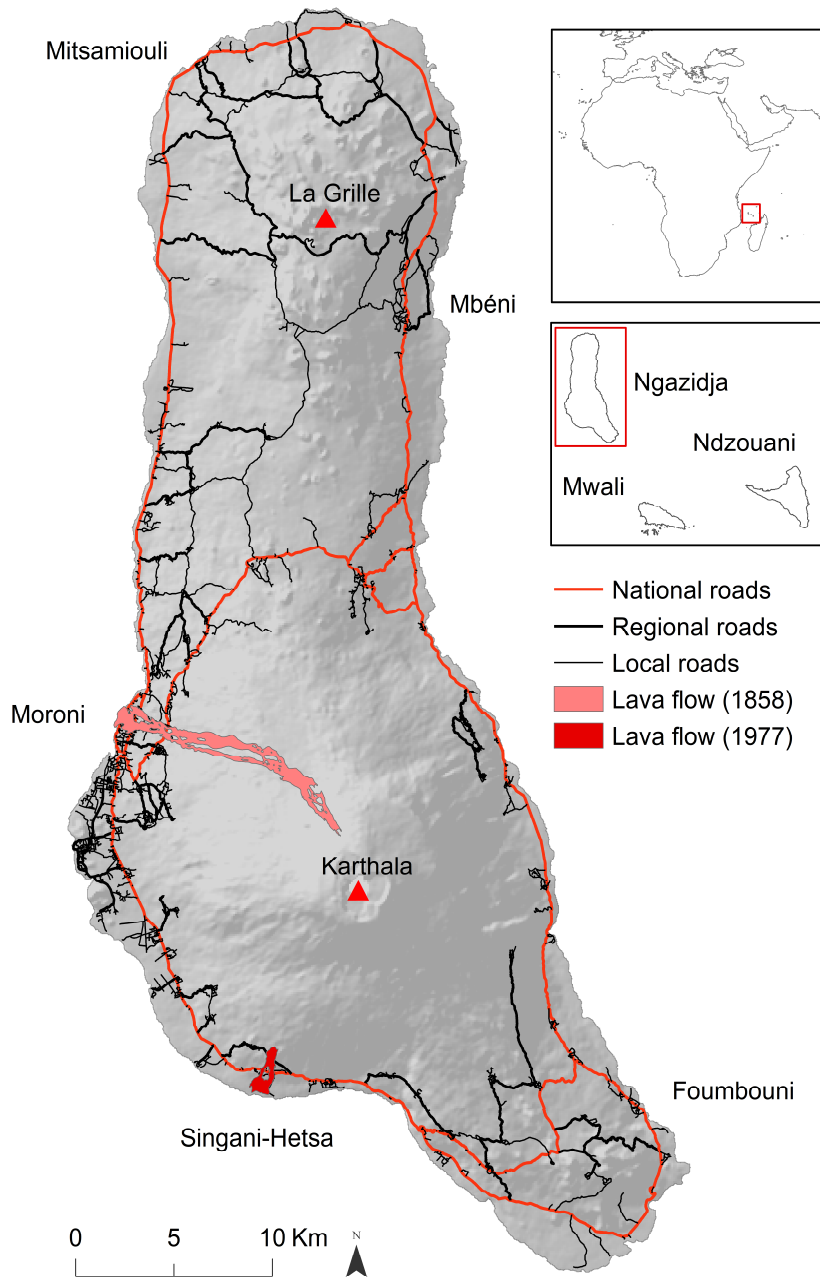
557 **14. Table Captions**

558 Table 1 – Lava flow hazard map input parameters implemented in Q-LavHA.

559

Table 2 – Lava flow hazard map input parameters implemented in Q-LavHA.

	Parameters	Value
Input file	Digital elevation model (m)	90
Lava flow propagation	$H_c$ (m)	3
	$H_p$ (m)	9
Lava flow length constraints	Mean length (m)	5200
	Standard deviation (m)	3200
Vent opening susceptibility map	Distance between the vents (m)	90
	Minimum probability to simulate	0
Simulation parameters	Number of iterations	500



565  
566  
567

Figure 1

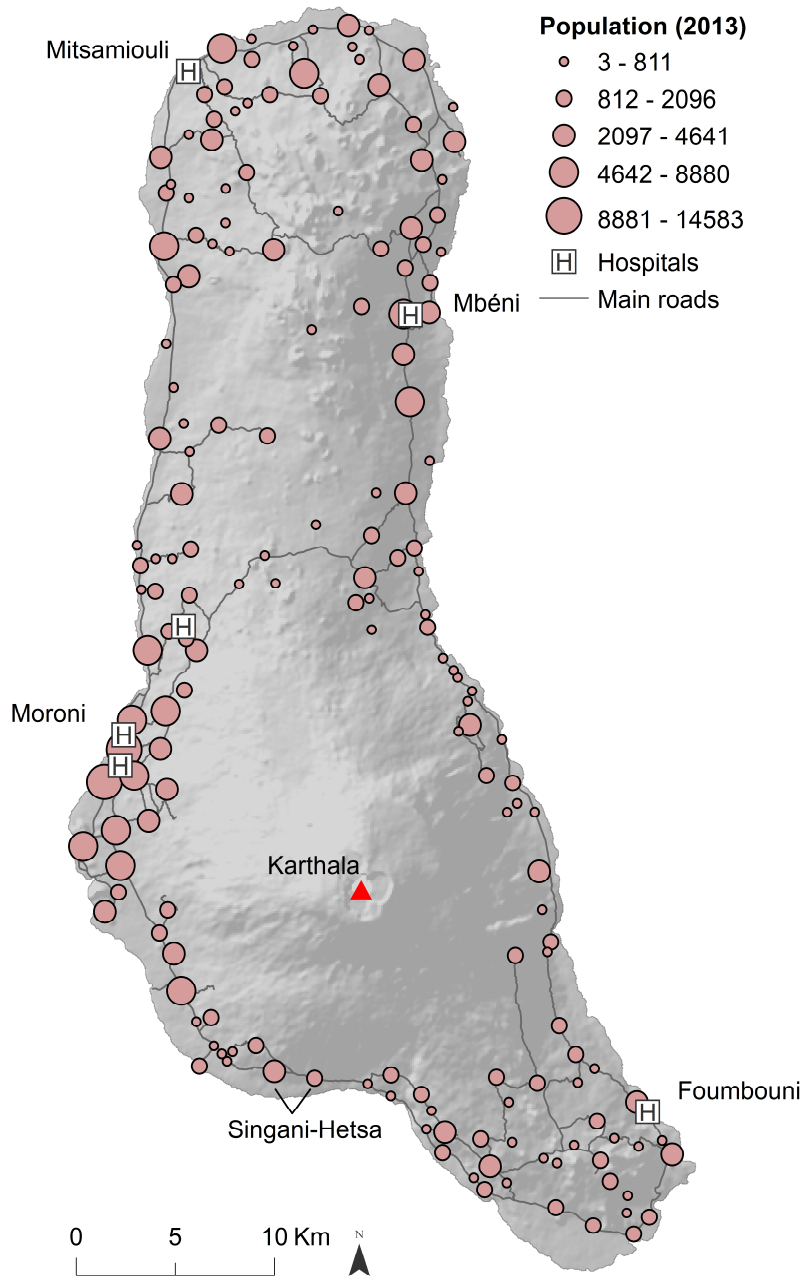
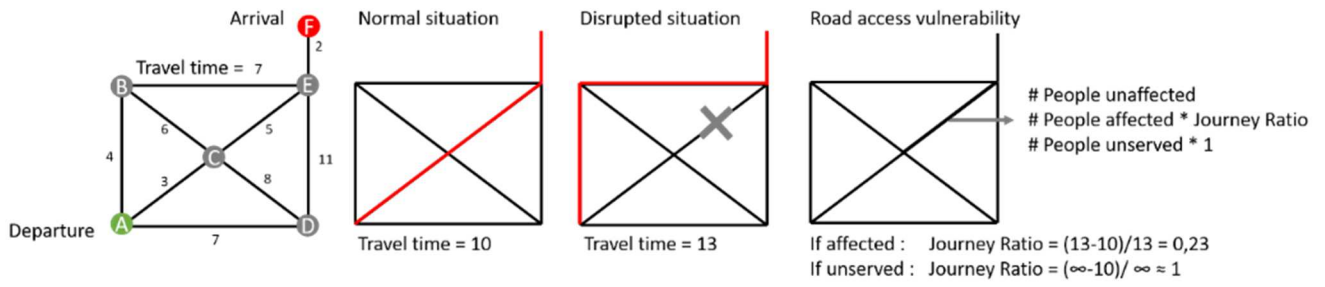


**Figure 2**

568  
569  
570  
571

572  
573  
574  
575

**Figure 3**



576

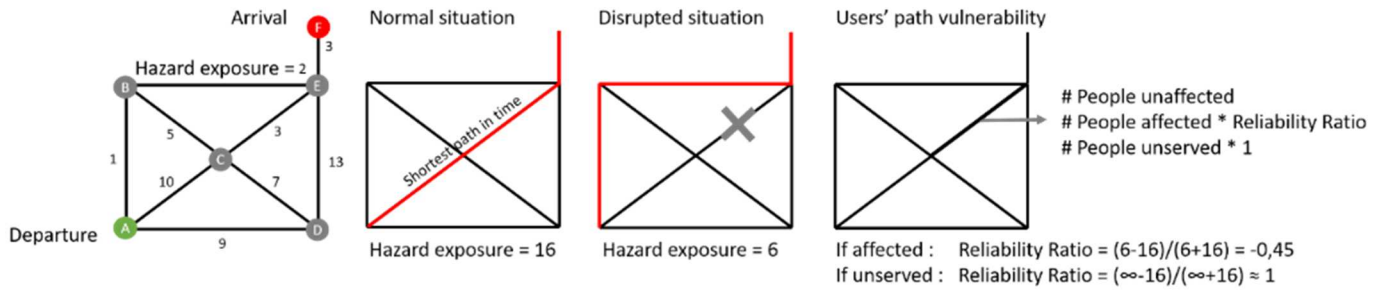
577

578

Figure 4

579

580



581

582

583

584

Figure 5

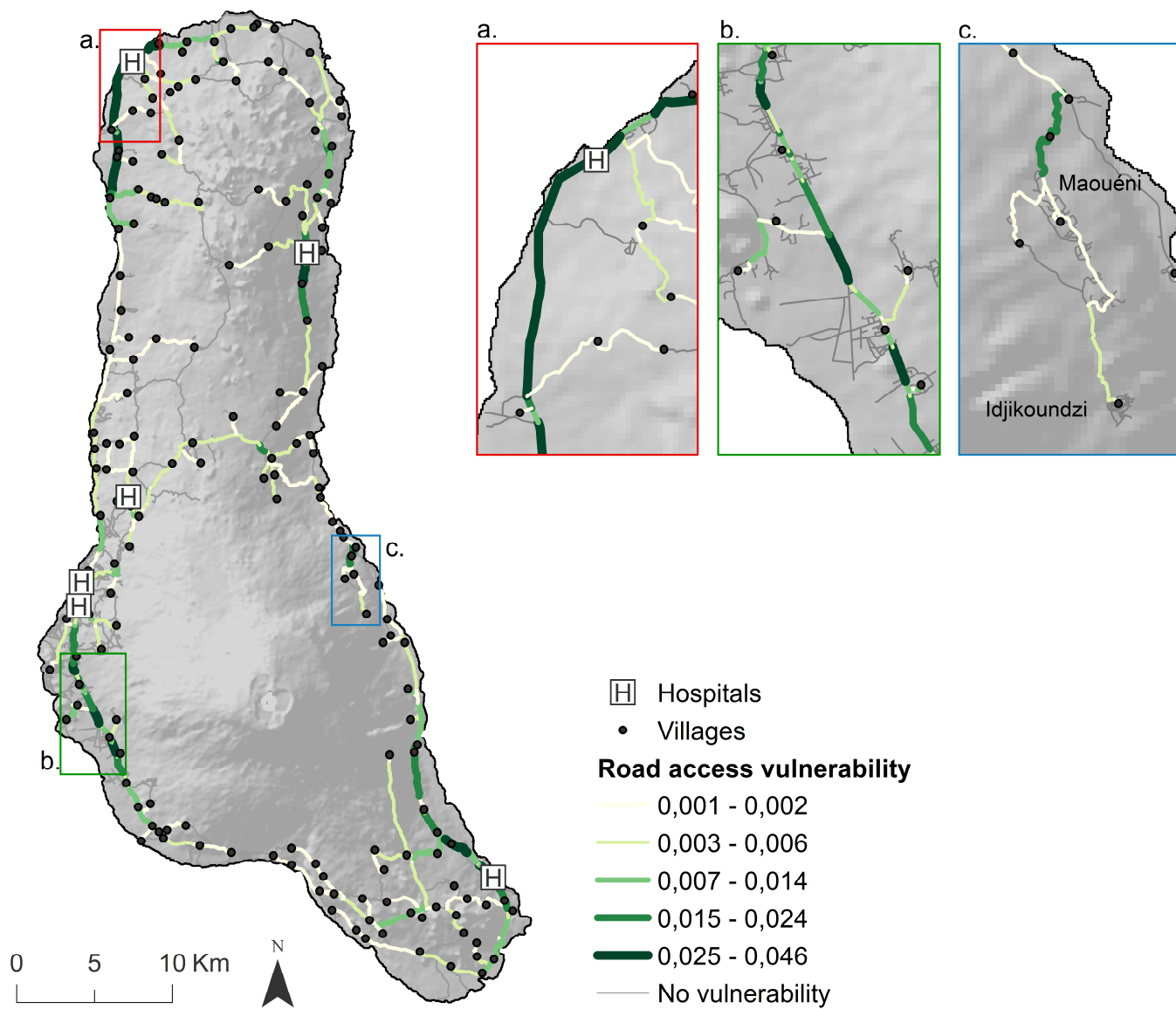
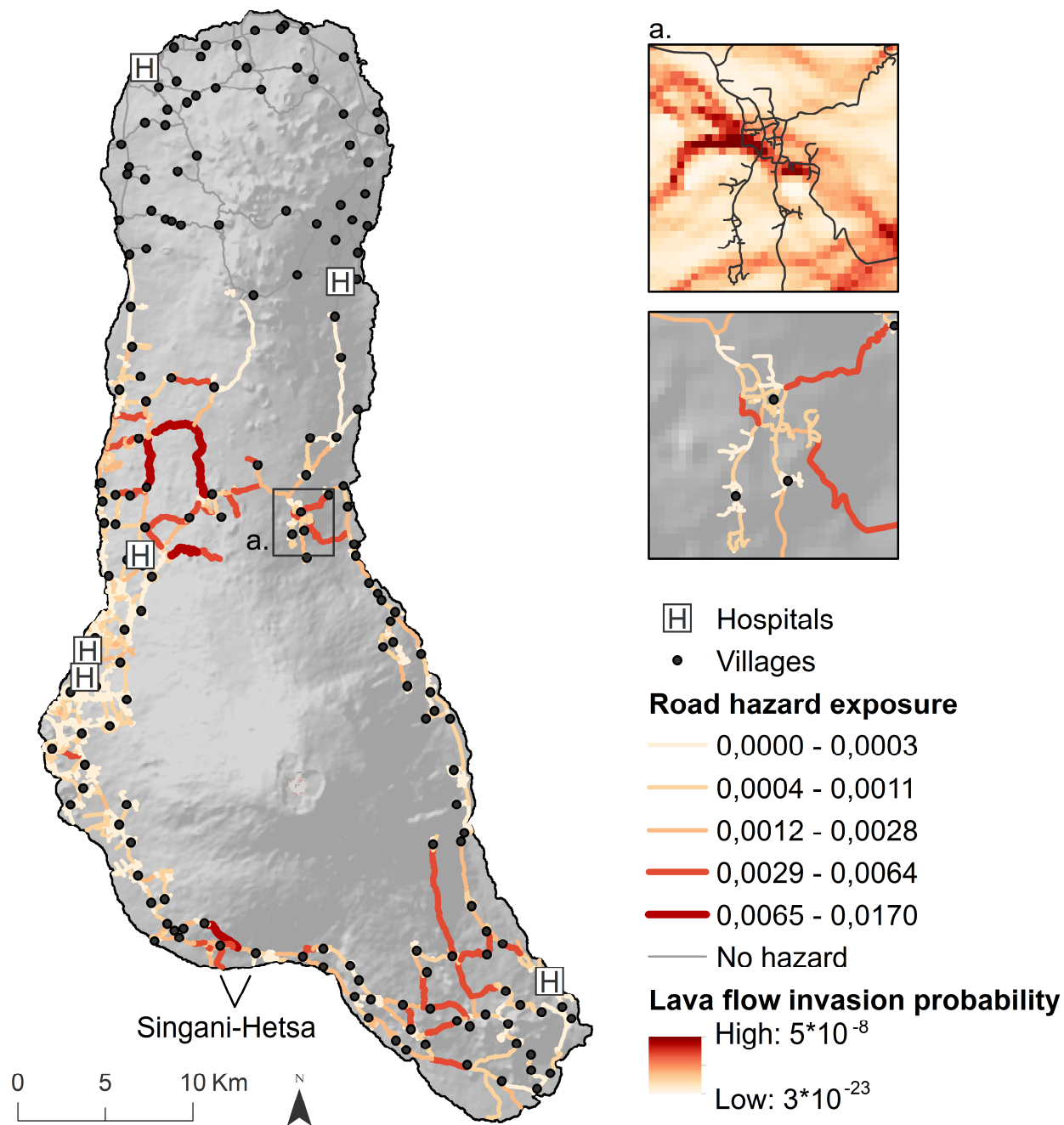


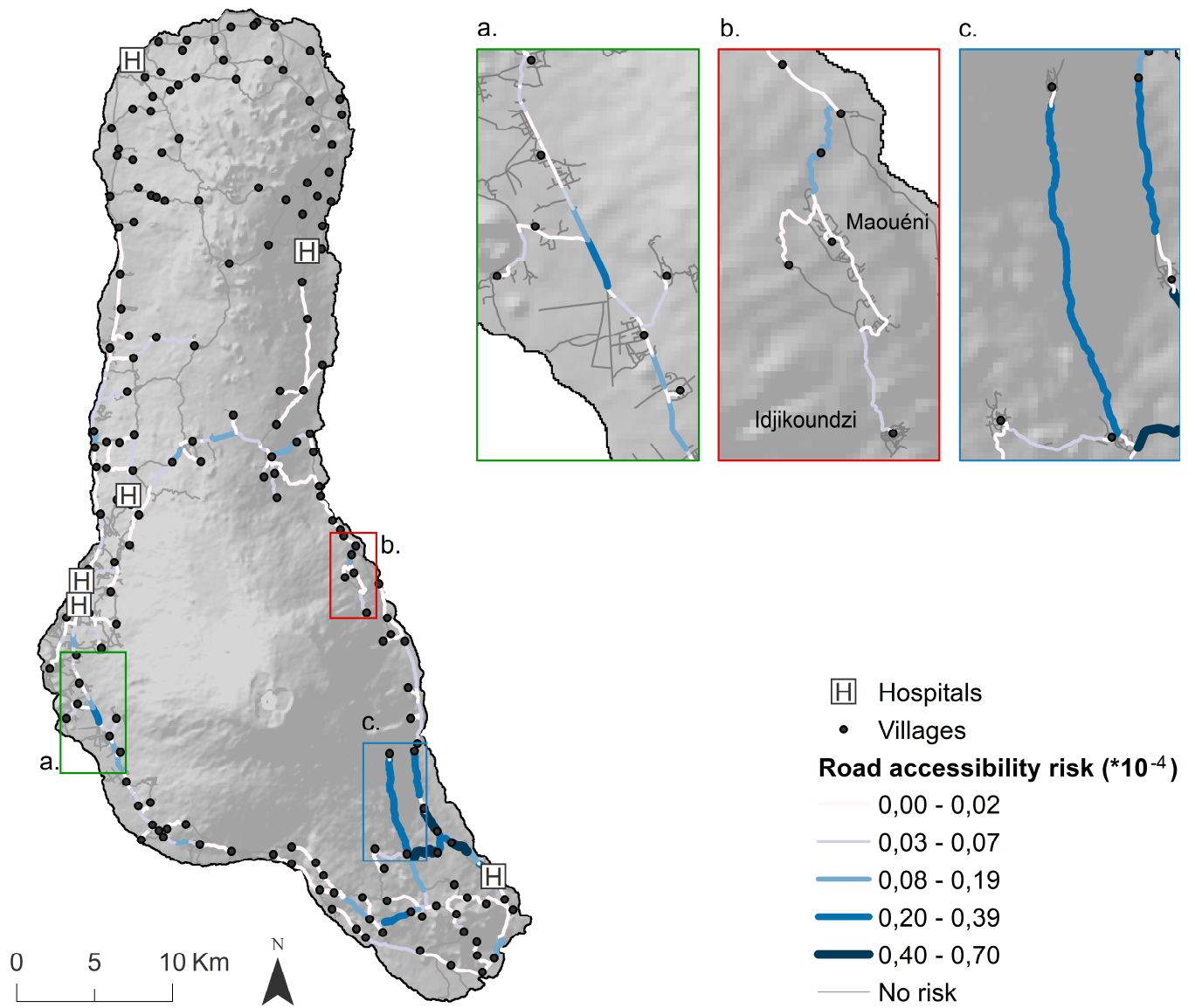
Figure 6

585  
586  
587  
588  
589



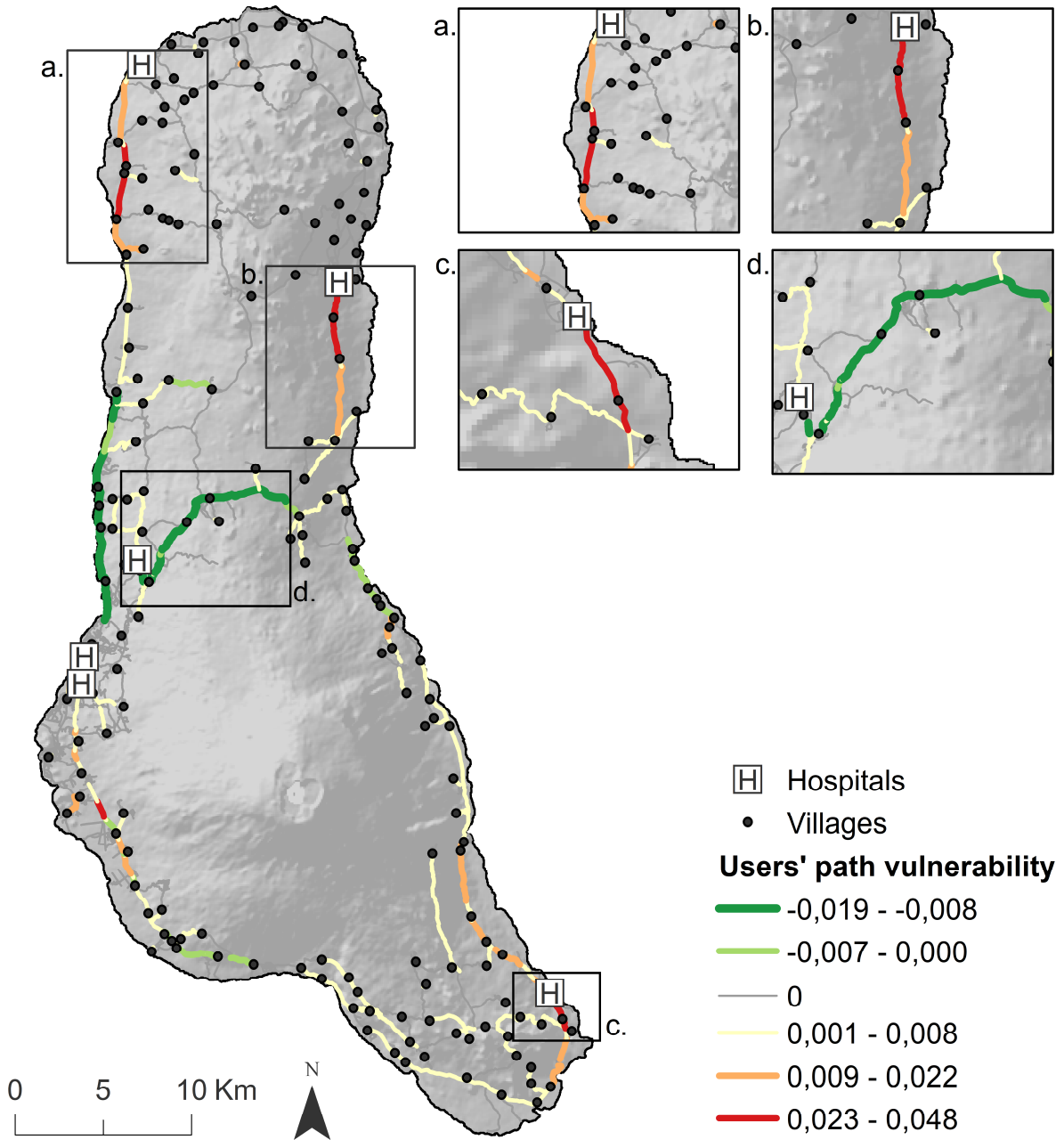
590  
591  
592

Figure 7



593  
 594  
 595  
 596  
 597  
 598

Figure 8

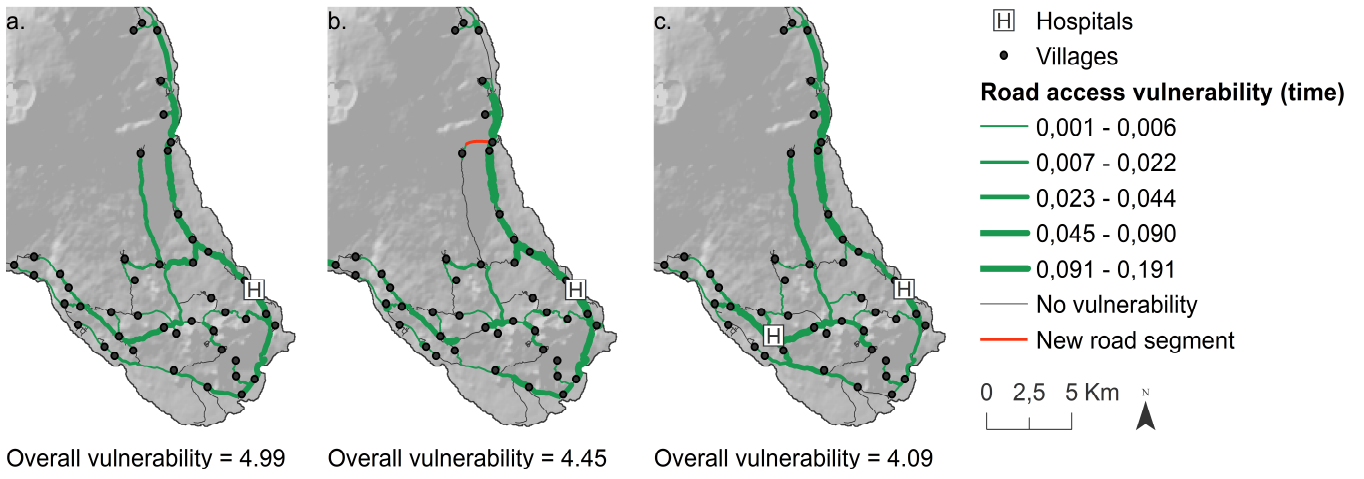


599  
600  
601  
602

Figure 9

603

604



605 Overall vulnerability = 4.99

606 Overall vulnerability = 4.45

607 Overall vulnerability = 4.09

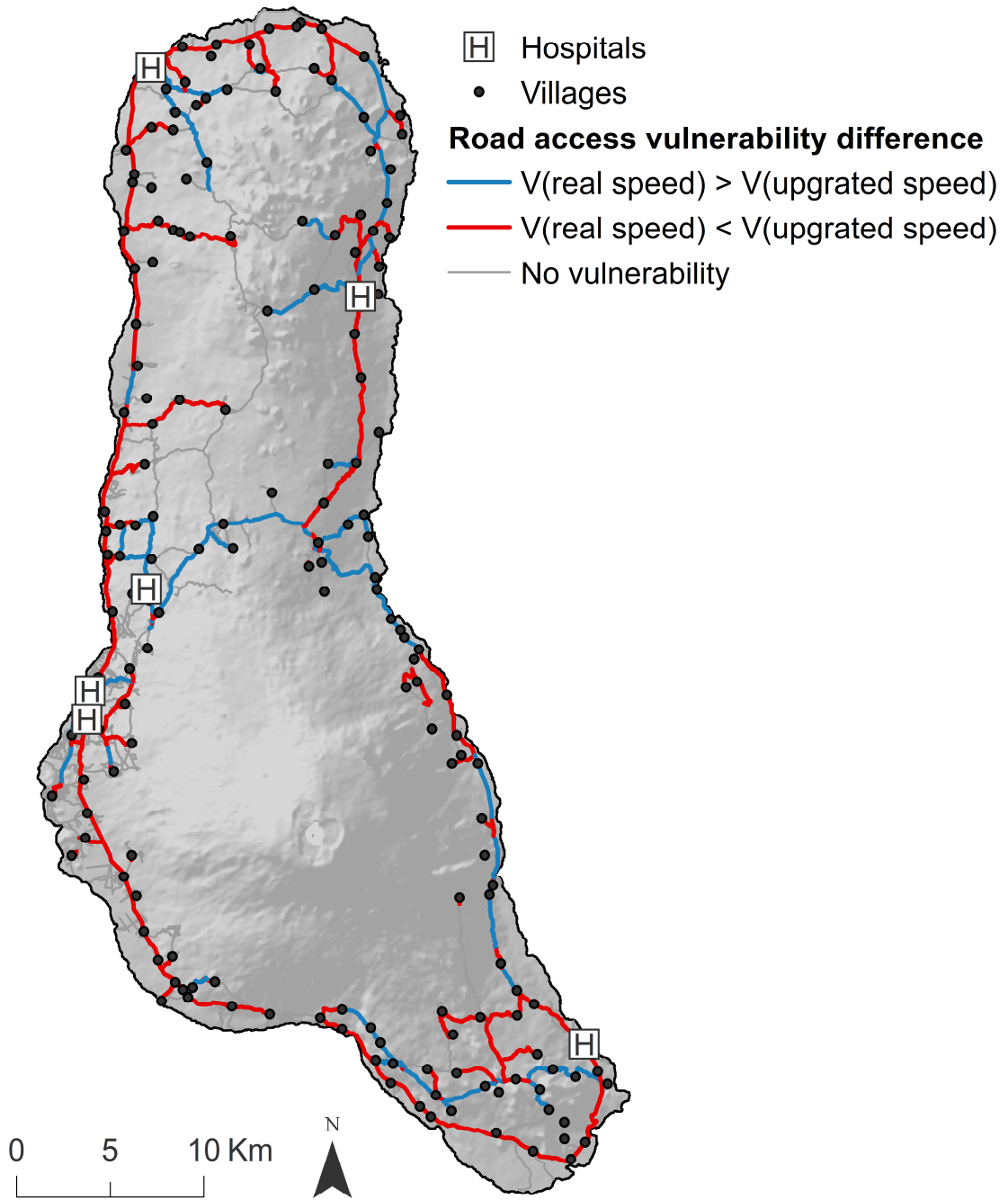
608

609

610

611

**Figure 10**



610

611

Figure 11